Do Photosynthetic Complexes Use Quantum Coherence to Increase Their Efficiency? Probably Not

Elinor Zerah Haursh,[1,2] Yonatan Dubi,[*1,2]

[1]Department of Chemistry and [2]Ilse-Katz Institute for Nanoscale Science and Technology, Ben-Gurion University of the Negev, Beer-Sheva 84105, Israel

[*]To whom correspondence should be addressed; E-mail: jdubi@bgu.ac.il.

Answering the titular question has become a central motivation in the field of quantum biology, ever since the idea was raised following a series of experiments demonstrating wave-like behavior in photosynthetic complexes. Here, we report a direct evaluation of the effect of quantum coherence on the efficiency of three natural complexes. An open quantum systems approach allows us to simultaneously identify their level of "quantumness" and efficiency, under natural physiological conditions. We show that these systems reside in a mixed quantum-classical regime, characterized by dephasing-assisted transport. Yet, we find that the change in efficiency at this regime is minute at best, implying that the presence of quantum coherence does not play a significant role in enhancing efficiency. However, in this regime efficiency is independent of any structural parameters, suggesting that evolution may have driven natural complexes to their parameter regime in order to "design" their structure for other uses.

Introduction

In the photosynthetic process, energy is transferred from an antenna (where light is collected) to a reaction center (where the energy is converted to chemical energy, to be used later by the organism). Excitons -bound electron–hole pairs - are the energy carriers in the photosynthetic process, carrying the harvested solar energy from the antenna to the reaction center, through a network of Bacteriochlorophylls (BChls), the so-called exciton-transfer complex (ETC) (*1*). Interest in the dynamics of excitons in the ETC exploded over the last decade, following recent experiments, where ultrafast nonlinear spectroscopy signals showed long-lived oscillations (*2–8*). The discovery of coherent oscillations in ETCs pushed forward the hypothesis that in natural photosynthetic complexes, which are extremely efficient, quantum coherence in the presence of an environment is used to assist energy transfer, an idea that has generated much excitement (and debate) (*9–19*).

The problem can basically be summarized in two seemingly simple questions; (1) can quantum coherence exist during the biologic process of photosynthetic energy transfer? (2) if it does, is it used in some way by the natural system to enhance its efficiency? The latter question is actually more subtle, and perhaps better phrased as (see Fig. 1(a)): does the presence of quantum coherence adds any functional advantage, such that it played a role in the driving forces that led, through evolution, to the current design of the natural photosynthetic apparatus?

Many theoretical (and experimental) works have addressed these questions, yet the question in the title remains largely unanswered. One reason is that while experiments are performed in vitro with coherent (pulsed) light, natural systems operate under very different conditions, namely continuous incoherent excitation (*18, 20–24*), and observing coherence under natural conditions is a very challenging task. That and more, it is hard to make the connection between the observed experimental findings and the energy transfer *efficiency*, which is related to the to-

tal rate at which energy can flow from the antenna to the reaction center (two ingredients which are essentially absent in the experiments).

Here we address the aforementioned questions, using tools developed from the theory of open quantum systems. Our approach allows us to evaluate efficiency directly while taking relevant physical parameters into account, and provides a simple way to estimate if the system is "quantum" or "classical", i.e. to evaluate whether environment-induced dephasing has pushed the system into the classical regime. We find that the answers to the questions posed above are "yes" and "no", namely that the excitonic system is indeed in the quantum-coherent regime (even for fast dephasing of ~ 100fs (*25*)), but that quantum coherence has only a minute effect on transport efficiency. Put simply, our findings suggest that the answer to the question posed in the title is negative.

Methods

The approach we take enables us to calculate both the total exciton current through the ETC, and the exciton population at each BChl site simultaneously, under the condition of continuous incoherent excitaions (*23, 24*), with physiologically relevant parameters. The joint evaluation of both currents and populations allows us to answer the questions posed in the introduction. First, the exciton current is a direct measure of the ETCs efficiency. This is easy to understand; the efficiency is simply the ratio between power output and power input. The power input is constant, and the power output is essentially the exciton energy times the exciton current.

Second, the populations allow us to evaluate the level of "quantumness" of the system. This was recognized in recent work (*26*), where a connection between exciton population, dephasing rate and the approach to classicality was established, through the mechanism of environment-assisted quantum transport (ENAQT). When an environment acts on a disordered quantum network (such as the exciton transfer complex), it induces a finite dephasing time. ENAQT is the

situation where the dependence of quantum transport on the dephasing rate is non-monotonic, showing a maximum at some optimal dephasing rate, and was considered to be a possible mechanism for the high efficiency of photosynthetic complexes (*27, 27–42*). The relation between ENAQT and particle populations is as follows . At the quantum regime (very small dephasing rate), the populations are essentially determined by the Hamiltonian structure of the network and the positions of the source and drain (antenna and reaction center in photosynthetic complexes). As dephasing rate increases, it reduces the variations in populations, so-called "population uniformization", flattening the population distribution, and resulting in an increase in current, which reaches a maximum at some optimal rate. For high dephasing rates, the system becomes essentially classical, and the populations are organized according to Fick's law, i.e. the formation of a uniform gradient between the source and drain. It is this gradient which can be used to define how "classical" is the system; once the gradient is fully formed (such that increasing the dephasing rate no longer changes the populations), one can say that the system is classical. The population uniformization mechanism is depicted in Fig. 1(b).
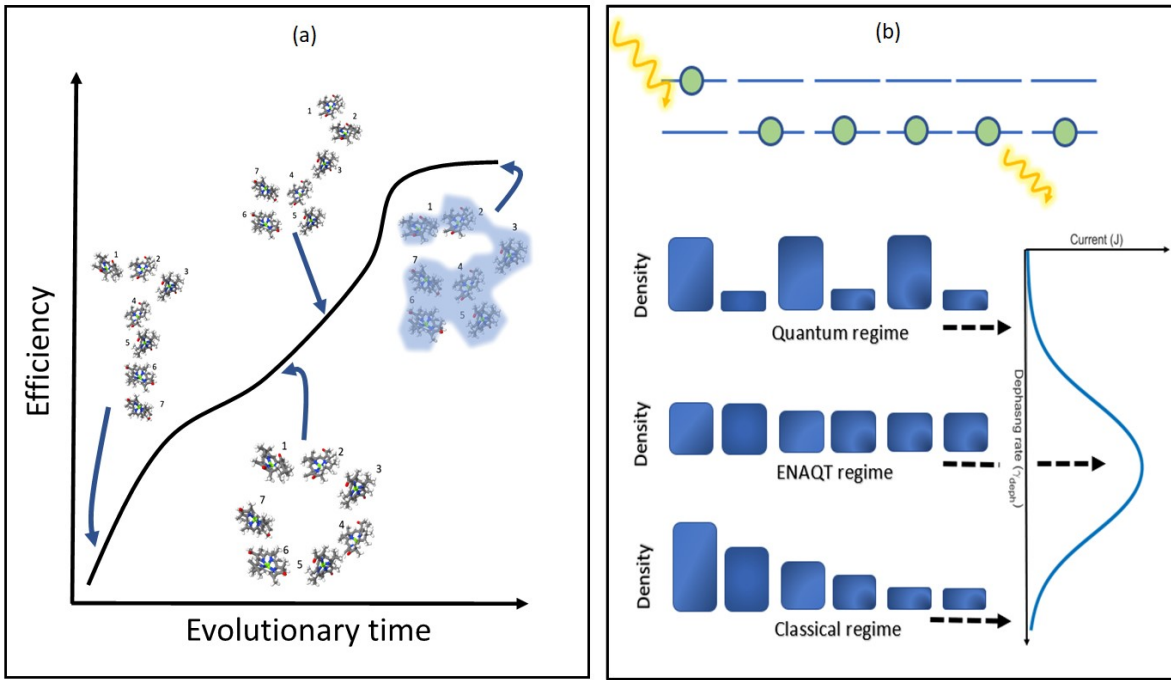
Figure 1: Mechanisms of efficiency-driven evolution and environment-assisted quantum transport. (a) Schematic description of the evolutionary progress of photosynthetic complexes towards their current geometry, with efficiency being the evolutionary driving force. As evolution progresses, the structure of the photosynthetic complex evolves towards its current structure (the FMO complex in this example), while increasing efficiency. Is this indeed the evolutionary pathway of photosynthetic complexes, and if so is quantum coherence part of the efficiency enhancement is a central question in the field of quantum biology. (b) Schematic depiction of the population uniformization mechanism shown for a uniform chain of six sites (Blue lines depict the sites in the chain, Yellow arrows show the excitation of first site and extraction from fifth site). The density of the sites are described by blue bars for the quantum regime, ENAQT regime and classical regime, along with a schematic form for the current vs dephasing curves.

In what follows, we evaluate both the transfer efficiency and populations from the Linbdlad quantum master equation (43), taking physically-relevant parameters (detailed form of the Lindblad equation is given in the SM section I). The dephasing rate serves as a free parameter in the calculations, but can be evaluated from experiments to be in the range of 10-10^3 femtoseconds. (2–7).

5

We consider three different photosynthetic exciton transfer complexes; the Fenna-Matthews-Olson (FMO) complex which appears in Green sulfur bacteria, the PC-645 protein, which is a sub-unit of the photosynthetic apparatus in cryptophyte algae, and LH2, part of the photosynthetic apparatus of the purple photosynthetic bacterium *Rhodopseudomonas acidophila* (their schematic structures are plotted in the insets to Figs.2 (a), 2 (b) and 4, respectively). All three complexes were shown to exhibit coherent energy-transfer oscillations in non-linear 2D spectroscopy measurements (*2, 6, 11, 44–48*). The Hamiltonian parametrization of each complex was taken from previous literature (*49–53*), and are provided in the SM (section I). Some crystallographic measurements suggest an updated model of the FMO complex, containing eight bacteriochlorophylls (Bchls) instead of seven (*54, 55*), a structure which has been parametrized and studied in the context of FMO energy transfer (e.g. (*56–58*)). Here we chose to focus on the seven Bchls model, as previous works demonstrated that the expected difference between the two models would be insignificant (*57, 58*).

The remaining parameters which are needed to fully define the parameter set are injection and extraction rates, i.e. the rate at which excitons are pushed into the ETC and extracted to the reaction center. The extraction rate can be estimated by considering the time-scales of different transport processes that take place in the photosynthetic complexes. For instance, the exciton transfer time between adjacent LH2 complexes was found to be $3 - 100$ps (*3, 11, 14, 18, 45, 53, 59*), and the trapping time of energy by the core complexes in PC-645 was found to be ≈ 100ps (*60*) We then set the extraction rate to an average of $\gamma_{ext} = 0.1$ ps^{-1}. However, a range of extraction rates was tested, and our results and conclusions are essentially insensitive to the extraction rate, as long as it is much larger than the injection rate (see below).

The injection (or excitation) rate is limited by the absorption cross section, which was estimated for by evaluating that there are $\sigma \sim 14$/s (14 excitons per second) for biological intensity of $I \sim 18\frac{W}{m^2}$ (*61*). The sunlight intensity can be as high as $I_{max} \sim 1300\frac{W}{m^2}$ (on a bright day

at the equator), which can be absorbed by $N \approx 400$ complexes in one vesicle (*62, 63*). The resulting *upper limit* for the injection rate is then $\gamma_{inj} = N \times \sigma \times I_{max}/I \sim 0.4\mu\mathrm{s}^{-1}$. We note that we have used the same injection rate for all organisms here, although FMO probably does not absorb energy directly from the sun. However, we considered the maximum injection rate that can obtained from the baseplate. This ensures that our results are correct even for extreme conditions (i.e. give an upper bound).

Results

Currents and populations in FMO and PC-645

With all parameters set, one can now evaluate the effect of the environment on the photosynthetic transfer efficiency. In Fig. 2 we plot the exciton current as a function of dephasing rate, for the FMO complex (a) and the PC-645 complex (b). Insets are the schematic structures of the complexes, respectively. The similarity between the plots is an indication for the relative insensitivity of the current to the internal structure Hamiltonian (*64*). The green-shaded area in Fig.2 shows the region of physiological dephasing rates. The ENAQT effect is clearly visible, as the current shows a maximum in the dephasing rate. However, the enhancement in the current due to dephasing is minute, constituting only ~ 0.0015 percent increase (even taking extreme values for the injection and extraction rates yields an ENAQT enhancement of only a few percent, see SM Section III). It seems unlikely that such a small efficiency enhancement would be a meaningful evolutionary driving force; it is more likely that other factors were prominent in the evolutionary design of these photosynthetic complexes.
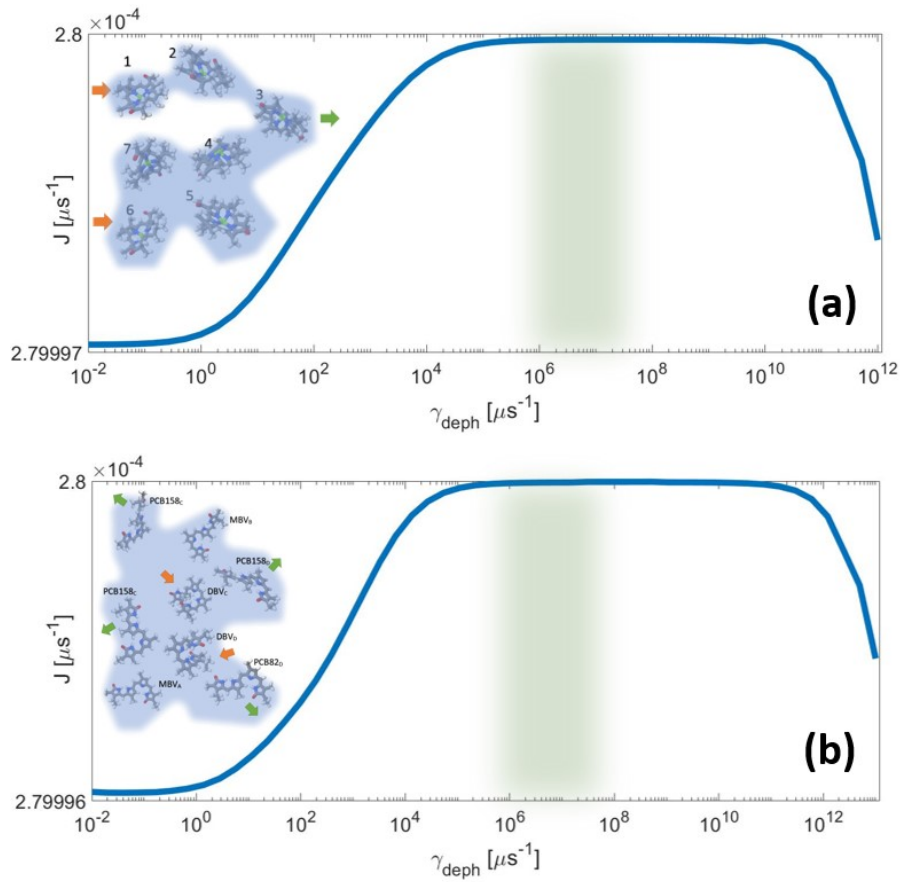
Figure 2: Calculated exciton current as a function of dephasing for the FMO (a) and pc-645 (b) complexes. The shaded Green area indicates the estimated range of physiological dephasing rates. Insets show a schematic description of the exciton complexes (the full Hamiltonians used are provided in the SM section VI).

The structure of the current-dephasing rate dependence already gives a hint that both FMO and PC-645 operate in the ENAQT regime under natural conditions. This can be further corroborated by looking at the exciton populations within the transfer complex for different dephasing rates. As pointed above, the three regimes (quantum, ENAQT and classical regimes) have very distinct features; the quantum regime is characterize by a spread of the populations determined by the structure of the Hamiltonian, the ENAQT regime by uniform populations, and the clas-

sical regime by a linear population gradient from source to drain.

In Fig. 3 the exciton population of the FMO complex is plotted for three values of dephasing rate, corresponding to the quantum ($\gamma_{deph} = 10^{-4}\mu s^{-1}$), biological conditions (ENAQT regime, $\gamma_{deph} = 10^{6}\mu s^{-1}$) and classical regime ($\gamma_{deph} = 10^{12}\mu s^{-1}$). Fig. 3(a) shows the occupation as a function of site number, but since the FMO is not a simple linear chain, in Fig. 3(b-d) we show the population on the FMO lattice, color-coded such that brighter colors represent lower density.

One can clearly observe the population uniformization that leads to ENAQT; In the quantum regime, populations seem disordered, and are determined by the interplay between the structure of the wave-functions and the source and drain positions. At intermediate dephasing, the population is essentially uniform, and a uniform gradient is formed between source and drain (sites 6 and 3) for strong dephasing.
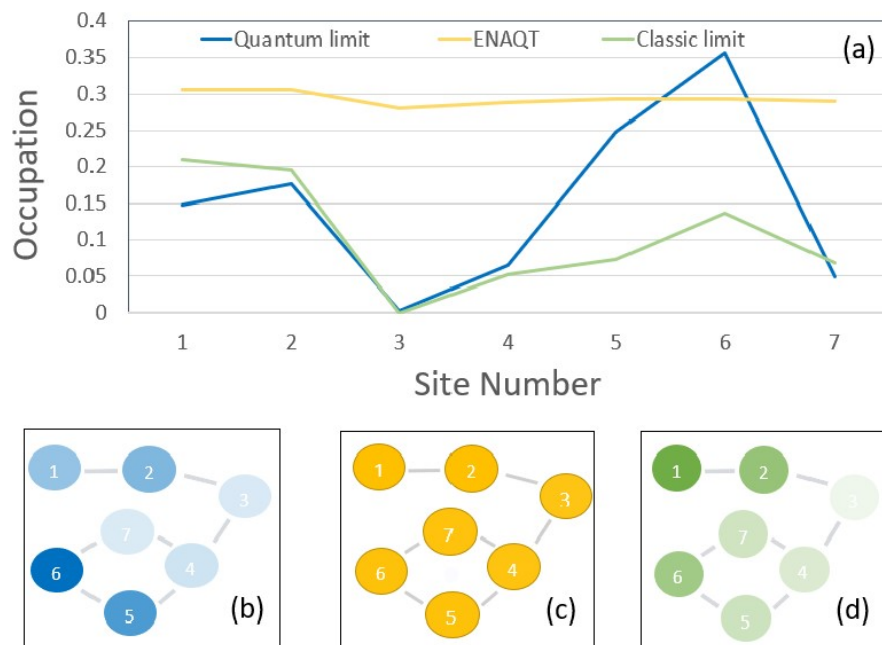
Figure 3: Calculated exciton current as a function of dephasing for the FMO (a) and pc-645 (b) complexes. The shaded Green area indicates the estimated range of physiological dephasing rates. Insets show a schematic description of the exciton complexes (the full Hamiltonians used are provided in the SM section VI).

ENAQT in LH2

In the LH2 complex, making the connection between ENAQT and population (i.e. recognizing the diffusive regime by observing a population gradient) is harder, because there is no simple spatial separation between the antenna (injection sites) and reaction center (source site) such that a gradient can be identified. As depicted in the inset of Fig. 4, the LH2 complex is composed of two rings of BChl pigments, B800 (yellow ring) and B850 (blue ring), named after

their energy absorption resonance (in nm), connected by a ring of Lycopen molecules (gray, long molecules) that absorb energy in the visible region of the spectrum (*51, 65–67*). Each of these parts can absorb light that excites an exciton that later would be transferred from one of the rings to the reaction center (*53, 59, 66*). The structure thus enables the occurrence of many exciton transfer paths. Nevertheless, a current vs dephasing curve for LH2 can still reveal the importance (or lack thereof) of coherence in transport.

In order to evaluate the efficiency of energy transfer in LH2 and its dependence on the dephasing rate, we calculate the excitonic current through LH2, considering multiple paths. Specifically, we assume that an exciton can be excited and extracted in any one of the BChl or molecular sites. In Fig. 4 we plot current as a function of dephasing rate for the LH2 system. Light pink lines are examples of specific paths, and the solid black line is the average curve (green area again marks the regime of physiological dephasing rates). In similarity to the cases of FMO and PC-645, one can see that indeed there is ENAQT, i.e. an increase in the exciton current, and that it is very small, ~ 0.05 percent. Similar results are obtained if multiple exciton injection and extraction are considered or if the exitations are of ring eigenstates (see SM, sections IV and V).
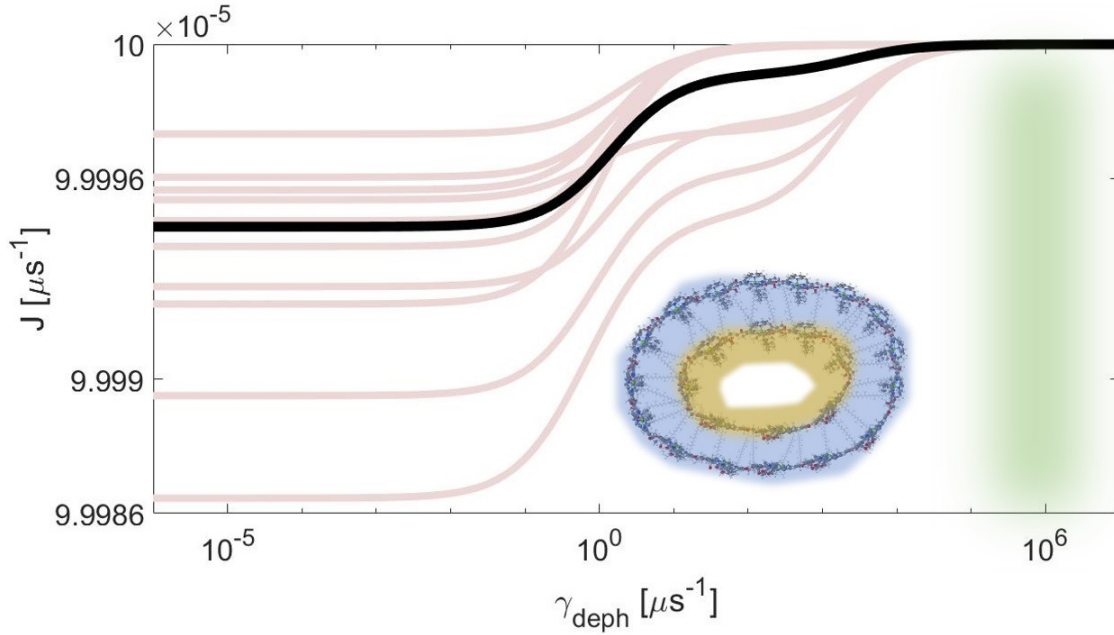
Figure 4: Density configuration (i.e. exciton occupation at different sites) of the FMO complex for three different regimes: quantum limit (blue line, $\gamma_{deph} = 10^{-4}\mu s^{-1}$), biological condition (yellow line, $\gamma_{deph} = 10^{6}\mu s^{-1}$) and quantum limit (green line, $\gamma_{deph} = 10^{12}\mu s^{-1}$). The transition from the quantum regime towards the classical regime is accompanied by a shift in the density configuration, from a wave-function-determined configuration to a uniform gradient between the source and sink, with a uniform configuration in between (*26*). To see this more clearly, figures (b)-(c) present the schematic structure of FMO, where each sphere represents a BChl site, and the color brightness reflects its relative density.

Discussion: Current, coherence and classicality

Figs 2 and 4 establish that there is no significant increase in the exciton current (and hence the efficiency) when comparing the fully quantum case (zero dephasing rate) and the physiological realistic dephasing rates ($10^6 - 10^8 \mu s^{-1}$).

Before discussing the relation between our results and the question in the title, we wish to elaborate further on the notion of "quantum" vs "classical". What makes the system "classical"?

As pointed above, one definition would be the onset of a population gradient, i.e. classical diffusion and Fick's law (*26*), but this is an operational definition, which ignores the presence of coherences (off diagonal terms of the density matrix) (*19*). Formally, coherence is necessary for observing current, because the current is proportional to (the imaginary part of) the off-diagonal elements of the density matrix, e.g., coherences. Thus, coherences are present also in the classical regime.

What really defines a "classical" system is not the lack of any coherence, but rather the fact that in a classical system, the coherences can be fully determined from the populations, without any additional information required. This implies no "long range" coherence, in the sense that sites which are not connected via hopping matrix elements in the Hamiltonian will have no coherence between them (i.e. no off-diagonal elements connecting them in the density matrix). This distinction between quantum and classical dynamics was quantified in Ref. (*9*), where the authors compared the local currents as derived from the off-diagonal density-matrix elements (i.e. quantum flux), $J_{ij}^Q = -2t_{ij}\Im(\rho_{ij})$ and from the diagonal elements (classical flux) $J_{ij}^C = \kappa_{ij}(\rho_{ii} - \rho_{jj})$ (where t_{ij} is the hopping matrix element between sites i and j, ρ is the density matrix and κ_{ij} is the classical exciton hopping rate between sites i and j, see SM for further details). In a "classical" regime, the two currents would be the same, implying that quantum coherences carry no additional information over the classical dynamics. This is what was found in Ref. (*9*) for the FMO complex.

Going back to our results, as can be clearly seen, there is a substantial drop in current when going towards very high dephasing rates. This occurs because in the classical regime, the system becomes diffusive, with a diffusion coefficient that is proportional to $\sim \bar{t}^2/\gamma_{deph}$ ($\bar{t}$ is some typical hopping matrix element) (*68*). The reduction of current with increasing γ_{deph} (but never to zero) is simply due to the decrease in the diffusion coefficient.

One could then argue that the intermediate dephasing rates observed in natural systems hold a

substantial advantage over much higher dephasing rates. Since the system is "fully classical" at such high rates, but has substantial quantum coherence in the ENAQT regime, one would then argue that in fact quantum effects are very important in determining the efficiency. Put differently, one could say that evolution drove the design of the light-harvesting system (in structural parameters such as geometry, orientation, etc.) away from the classical regime in order to increase its exciton transfer efficiency.

To counter this argument, we note that the drop in current occurs at unrealistically high dephasing rates, which means that the inherent system parameters would have to be tuned (by evolution) in such a way that pushes the system to the classical regime in physiological dephasing times. However, we find that the regime of ENAQT is extremely robust, and depends very weakly on the Hamiltonian parameters (this can also be seen by the similarity between the FMO and PC-645 systems), in line with existing literature (*69–72*).

This can be understood by analyzing, for instance, the analytical expressions for currents and populations of linear uniform models (*26*) (see SI section II). What we find is that the ENAQT regime is confined to the regime of $\gamma_{inj} < \gamma_{deph} < \frac{2\bar{t}^2}{\gamma_{inj}}$, where $\bar{t}$ is some effective or average hopping matrix element (which can be determined from, e.g. the bandwidth of the quantum system), and assuming $\gamma_{inj} \ll \gamma_{ext}$. Since the injection and extraction rates are external parameters, changing the ENAQT regime would require substantial reduction in the hopping matrix elements, but this would reduce the ability of the system to transfer energy. Presumably, this is the reason all three complexes have similar ranges of hopping matrix elements.

This analysis implies that the ENAQT regime is really the "natural" regime at which these systems operate; faster dephasing would require dynamics which are much faster than those of the proteins surrounding the ETCs, while longer dephasing times would require lower temperatures or deeper isolation of the chromophores. Figs.1 and 3 demonstrate that, surprisingly, at the ENAQT regime the current reaches a maximum which is limited by the injection rate, and

14

is essentially independent of any Hamiltonian parameters.

To show this directly, in Fig. 5 we show the current-dephasing rate curves of over 5000 random realizations of FMO-like networks. In this calculation, the diagonal elements (which have an absolute value with insignificant contribution to current) and the injection and extraction positions are kept fixed, and the hopping matrix elements, which define the network structure, are distributed randomly in the regime of ± 200cm^{-1}. The currents at the quantum regime differ substantially, since they depend on the detailed wave-function structure of a given realization (some realizations have very weak coupling between the source and sink, resulting in small currents at the quantum regime). Similarly, at the classical regime there is a distribution of currents (since the onset of the classical regime is sensitive to the hopping elements, and hence changes between realizations). However, at the ENAQT regime, there is essentially *no dependence on the Hamiltonian parameters.* This means that no matter how the network is arranged, the current is the same. In different words, at the ENAQT regime, the value of the current is completely indifferent to the network structure. Therefore, an inevitable conclusion is that enhancing the current was *not* an evolutionary driver to determine the network structure.

This is not unique to the FMO complex. In fact, we find similar results for the PC-645 and LH2 complexes (not shown). Moreover, in the ENAQT regime the system is robust against not only geometrical changes, but also to many other parameters. As a specific example (one out of many), we consider the excitation points of LH2. The LH2 complex is coupled not only to external excitations (via direct light absorption) but also to excitation from neighboring complexes. To mimic this effect, in the inset of Figure 4 we plot the current-dephasing rate curves of the LH2 complex, taking a random number and position of injection and extraction sites (between two and four injection and extraction sites). Clearly, neither the number nor position of the injection sites affects the current in the ENAQT regime.

 The picture that emerges from the calculations presented here is as follows. The photosynthetic
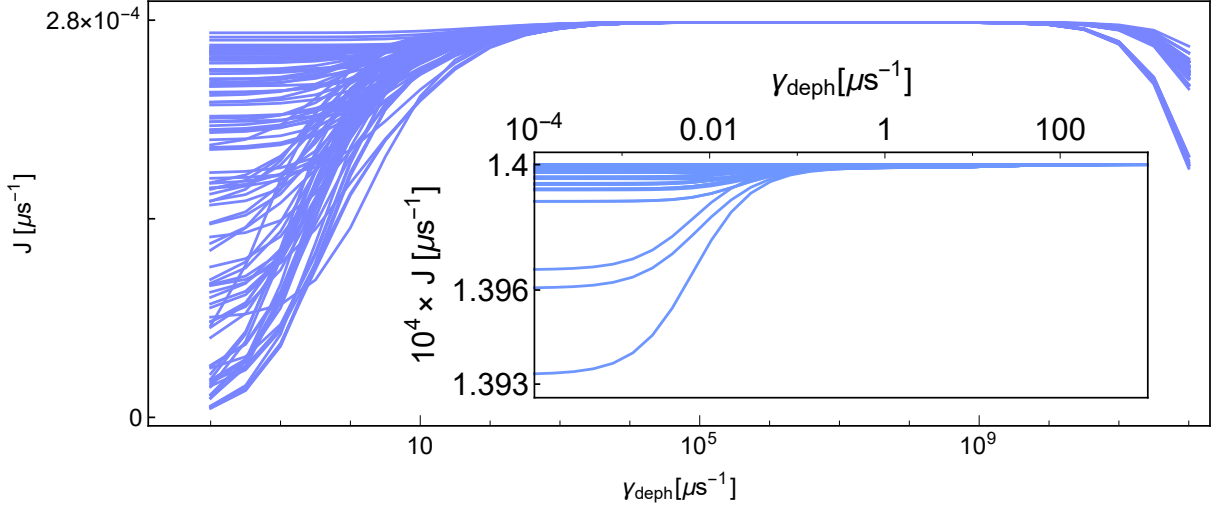
Figure 5: Density configuration (i.e. exciton occupation at different sites) of the FMO complex for three different regimes: quantum limit (blue line, $\gamma_{deph} = 10^{-4}\mu s^{-1}$), biological condition (yellow line, $\gamma_{deph} = 10^{6}\mu s^{-1}$) and quantum limit (green line, $\gamma_{deph} = 10^{12}\mu s^{-1}$). The transition from the quantum regime towards the classical regime is accompanied by a shift in the density configuration, from a wave-function-determined configuration to a uniform gradient between the source and sink, with a uniform configuration in between (*26*). To see this more clearly, figures (b)-(c) present the schematic structure of FMO, where each sphere represents a BChl site, and the color brightness reflects its relative density.

excitonic transfer networks, despite their structural differences, all operate in an environment with dephasing time τ_{deph} of a few hundred femtoseconds (up to 1ps), which puts them in the ENAQT regime. This regime is characterized by having an exciton current which is only slightly higher than the fully quantum regime, and reaches a maximum which is limited by the injection rate. The real advantage of being in the ENAQT regime is the surprising essential independence of the current on any particular structural parameters of the system. This leads to the conclusion that the structure of neither FMO, PC-645 or LH2 did not evolve in order to enhance efficiency (since it is essentially the same in all of them).

If anything, one could claim that evolution drove the physiological times to be what they are because in this regime the ETC network structure is irrelevant to efficiency, and hence can be used for a different function (stability, for instance (*16*)). However, one must also consider the

possibility that the physiological coherence time was also not part of the evolutionary driving, and developed by nothing more than a happy coincidence. Indeed, the physiological dephasing time seems to be a middle ground; faster coherence is typical to electronic systems but not to vibrational systems, and slower coherence times are unlikely in physiological environment. Therefore, two central challenges remain for future studies. The first is still to understand what determines the origin of the dephasing time τ_{deph} observed in experiments (e.g., (*73, 74*)), with the goal of understanding whether the observed values are somehow unique and could they be different. The second challenge is to look for other possible evolutionary advantages that the structures of the photosynthetic transfer complexes provide. Overcoming these challenges will push forward the understanding of the possible role of quantum effects in photosynthetic complexes.

Acknowledgments

Supplementary materials

Fig.s1. Current enhancement as a function of injection and extraction rates for FMO and pc-645

Fig.s2. Histogram of current enhancement from 10,000 different configurations of injection and extraction sites.

Fig.s3. Current as a function of dephasing rate for the case for excitation in the energy basis.

References

1. M. Mohseni, Y. Omar, G. S. Engel, M. B. Plenio, *Quantum effects in biology* (Cambridge University Press, 2014).

2. H. Lee, Y. Cheng, G. Fleming, Coherence dynamics in photosynthesis: protein protection of excitonic coherence. *Science* **316**, 1462-1465 (2007).

3. G. S. Engel, T. R. Calhoun, E. L. Read, T.-K. Ahn, T. Manal, Y.-C. Cheng, R. E. Blankenship, G. R. Fleming, Evidence for wavelike energy transfer through quantum coherence in photosynthetic systems. *Nature* **446**, 782-786 (2007).

4. T. R. Calhoun, N. S. Ginsberg, G. S. Schlau-Cohen, Y.-C. Cheng, M. Ballottari, R. Bassi, G. R. Fleming, Quantum coherence enabled determination of the energy landscape in light-harvesting complex ii. *The Journal of Physical Chemistry B* **113**, 16291-16295 (2009).

5. E. Collini, C. Y. Wong, K. E. Wilk, P. M. Curmi, P. Brumer, G. D. Scholes, Coherently wired light-harvesting in photosynthetic marine algae at ambient temperature. *Nature* **463**, 644–647 (2010).

6. G. Panitchayangkoon, D. Hayes, K. A. Fransted, J. R. Caram, E. Harel, J. Wen, R. E. Blankenship, G. S. Engel, Long-lived quantum coherence in photosynthetic complexes at physiological temperature. *Proceedings of the National Academy of Sciences* **107**, 12766-12770 (2010).

7. G. Panitchayangkoon, D. V. Voronine, D. Abramavicius, J. R. Caram, N. H. Lewis, S. Mukamel, G. S. Engel, Direct evidence of quantum transport in photosynthetic light-

harvesting complexes. *Proceedings of the National Academy of Sciences* **108**, 20908–20912 (2011).

8. R. E. Blankenship, D. M. Tiede, J. Barber, G. W. Brudvig, G. Fleming, M. Ghirardi, M. Gunner, W. Junge, D. M. Kramer, A. Melis, *et al.*, Comparing photosynthetic and photovoltaic efficiencies and recognizing the potential for improvement. *science* **332**, 805–809 (2011).

9. J. Wu, F. Liu, J. Ma, R. J. Silbey, J. Cao, Efficient energy transfer in light-harvesting systems: Quantum-classical comparison, flux network, and robustness analysis. *Journal of Chemical Physics* **137**, 174111 (2012). Publisher: American Institute of Physics.

10. R. d. J. Leon-Montiel, I. Kassal, J. P. Torres, Importance of excitation and trapping conditions in photosynthetic environment-assisted energy transport. *The Journal of Physical Chemistry B* **118**, 10588–10594 (2014).

11. H. W. Rathbone, J. A. Davis, K. A. Michie, S. C. Goodchild, N. O. Robertson, P. M. Curmi, Coherent phenomena in photosynthetic light harvesting: part two—observations in biological systems. *Biophysical Reviews* **10**, 1443–1463 (2018).

12. G. Fleming, S. Huelga, M. Plenio, Focus on quantum effects and noise in biomolecules. *New Journal of Physics* **13**, 115002 (2011).

13. I. Kassal, J. Yuen-Zhou, S. Rahimi-Keshari, Does coherence enhance transport in photosynthesis. *J. Phys. Chem. Lett.* **4**, 362–367 (2013).

14. H.-G. Duan, V. I. Prokhorenko, R. J. Cogdell, K. Ashraf, A. L. Stevens, M. Thorwart, R. D. Miller, Nature does not rely on long-lived electronic quantum coherence for photosynthetic energy transfer. *Proceedings of the National Academy of Sciences* **114**, 8493–8498 (2017).

15. A. Chenu, G. D. Scholes, Coherence in energy transfer and photosynthesis. *Annual review of physical chemistry* **66**, 69–96 (2015).

16. N. Keren, Y. Paltiel, Photosynthetic energy transfer at the quantum/classical border. *Trends in plant science* **23**, 497–506 (2018).

17. J. Cao, R. J. Cogdell, D. F. Coker, H.-G. Duan, J. Hauer, U. Kleinekathöfer, T. L. Jansen, T. Mančal, R. D. Miller, J. P. Ogilvie, *et al.*, Quantum biology revisited. *Science Advances* **6**, eaaz4888 (2020).

18. S. Bourne Worster, C. Stross, F. M. Vaughan, N. Linden, F. R. Manby, Structure and efficiency in bacterial photosynthetic light harvesting. *The journal of physical chemistry letters* **10**, 7383–7390 (2019).

19. P.-Y. Yang, J. Cao, Steady-state analysis of light-harvesting energy transfer driven by incoherent light: From dimers to networks. *Journal of Physical Chemistry Letters* **11**, 7204–7211 (2020). Publisher: American Chemical Society.

20. D. Manzano, Quantum transport in networks and photosynthetic complexes at the steady state. *PLOS ONE* **8** (2013).

21. K. M. Pelzer, T. Can, S. K. Gray, D. K. Morr, G. S. Engel, Coherent transport and energy flow patterns in photosynthesis under incoherent excitation. *The Journal of Physical Chemistry B* **118**, 2693–2702 (2014).

22. L. A. Pachón, J. D. Botero, P. Brumer, Open system perspective on incoherent excitation of light-harvesting systems. *Journal of Physics B: Atomic, Molecular and Optical Physics* **50**, 184003 (2017).

23. P. Brumer, Shedding (incoherent) light on quantum effects in light-induced biological processes. *The journal of physical chemistry letters* **9**, 2946–2955 (2018).

24. L. F. Morales-Curiel, R. d. J. León-Montiel, Photochemical dynamics under incoherent illumination: Light harvesting in self-assembled molecular j-aggregates. *The Journal of Chemical Physics* **152**, 074304 (2020).

25. E. Thyrhaug, R. Tempelaar, M. J. Alcocer, K. Žídek, D. Bína, J. Knoester, T. L. Jansen, D. Zigmantas, Identification and characterization of diverse coherences in the fenna–matthews–olson complex. *Nature chemistry* **10**, 780–786 (2018).

26. E. Zerah-Harush, Y. Dubi, Universal origin for environment-assisted quantum transport in exciton transfer networks. *The journal of physical chemistry letters* **9**, 1689–1695 (2018).

27. F. Caruso, A. W. Chin, A. Datta, S. F. Huelga, M. B. Plenio, Highly efficient energy excitation transfer in light-harvesting complexes: The fundamental role of noise-assisted transport. *The Journal of Chemical Physics* **131**, 105106 (2009).

28. P. Rebentrost, M. Mohseni, I. Kassal, S. Lloyd, A. Aspuru-Guzik, Environment-assisted quantum transport. *new journal of physics* **11**, 033003 (2009).

29. M. Mohseni, P. Rebentrost, S. Lloyd, A. Aspuru-Guzik, Environment-assisted quantum walks in photosynthetic energy transfer. *Journal of Chemical Physics* **129**, 174106 (2008).

30. A. W. Chin, A. Datta, F. Caruso, S. F. Huelga, M. B. Plenio, Noise-assisted energy transfer in quantum networks and light-harvesting complexes. *new journal of physics* **12**, 065002 (2010).

31. M. B. Plenio, S. F. Huelga, Dephasing-assisted transport: quantum networks and biomolecules. *new journal of physics* **10**, 113019 (2008).

32. I. Kassal, A. Aspuru-Guzik, Environment-assisted quantum transport in ordered systems. *new journal of physics* **14**, 053041 (2012).

33. F. Caruso, Universally optimal noisy quantum walks on complex networks. *New Journal of Physics* **16**, 055015 (2014).

34. Y. Li, F. Caruso, E. Gauger, S. C. Benjamin, "momentum rejuvenation" underlies the phenomenon of noise-assisted quantum energy flow. *New Journal of Physics* **17**, 013057 (2015).

35. A. Marais, I. Sinayskiy, A. Kay, F. Petruccione, A. Ekert, Decoherence-assisted transport in quantum networks. *New Journal of Physics* **15**, 013038 (2013).

36. I. Sinayskiy, A. Marais, F. Petruccione, A. Ekert, Decoherence-assisted transport in a dimer system. *Physical Review letters* **108**, 020602 (2012).

37. H.-B. Chen, N. Lambert, Y.-C. Cheng, Y.-N. Chen, F. Nori, Using non-markovian measures to evaluate quantum master equations for photosynthesis. *Scientific Reports* **5**, 12753 (2015).

38. Y. Dubi, Interplay between dephasing and geometry and directed heat flow in exciton transfer complexes. *Journal of Physical Chemistry C* **119**, 25252-25259 (2015).

39. G. P. Berman, A. I. Nesterov, G. V. Lopez, R. T. Sayre, Superradiance transition and non-photochemical quenching in photosynthetic complexes. *The Journal of Physical Chemistry C* **119**, 22289-22296 (2015).

40. S. Baghbanzadeh, I. Kassal, Distinguishing the roles of energy funnelling and delocalization in photosynthetic light harvesting. *Physical Chemistry Chemical Physics* **18**, 7459-7467 (2016).

41. J. Cao, R. J. Silbey, Optimization of exciton trapping in energy transfer processes. *Journal of Physical Chemistry A* **113**, 13825–13838 (2009).

42. M. Sarovar, A. Ishizaki, G. R. Fleming, K. B. Whaley, Quantum entanglement in photosynthetic light-harvesting complexes. *Nature Physics* **6**, 462–467 (2010).

43. H.-P. Breuer, F. Petruccione, *The theory of open quantum systems* (Oxford University Press on Demand, 2002).

44. E. Collini, C. Y. Wong, K. E. Wilk, P. M. G. Curmi, P. Brumer, G. D. Scholes, Coherently wired light-harvesting in photosynthetic marine algae at ambient temperature. *Nature* **463**, 644–647 (2000).

45. R. Hildner, D. Brinks, J. B. Nieder, R. J. Cogdell, N. F. v. Hulst, Quantum coherent energy transfer over varying pathways in single light-harvesting complexes. *Science* **340**, 1448–1451 (2013).

46. F. Ma, L.-J. Yu, R. Hendrikx, Z.-Y. Wang-Otomo, R. Van Grondelle, Excitonic and vibrational coherence in the excitation relaxation process of two lh1 complexes as revealed by two-dimensional electronic spectroscopy. *The journal of physical chemistry letters* **8**, 2751–2756 (2017).

47. M. Ferretti, V. I. Novoderezhkin, E. Romero, R. Augulis, A. Pandit, D. Zigmantas, R. van Grondelle, The nature of coherences in the b820 bacteriochlorophyll dimer revealed by two-dimensional electronic spectroscopy. *Physical Chemistry Chemical Physics* **16**, 9930–9939 (2014).

48. J. C. Dean, T. Mirkovic, Z. S. Toa, D. G. Oblinsky, G. D. Scholes, Vibronic enhancement of algae light harvesting. *Chem* **1**, 858–872 (2016).

49. M. Cho, H. M. Vaswani, T. Brixner, J. Stenger, G. R. Fleming, Exciton analysis in 2d electronic spectroscopy. *The Journal of Physical Chemistry B* **109**, 10542–10556 (2005).

50. B. Hein, C. Kreisbeck, T. Kramer, M. Rodríguez, Modelling of oscillations in two-dimensional echo-spectra of the fenna–matthews–olson complex. *New journal of physics* **14**, 023018 (2012).

51. S. Tretiak, C. Middleton, V. Chernyak, S. Mukamel, Exciton hamiltonian for the bacteri-ochlorophyll system in the LH2 antenna complex of purple bacteria. *Journal of Physical Chemistry B* **104**, 4519–4528 (2000).

52. S. Tretiak, C. Middleton, V. Chernyak, S. Mukamel, Bacteriochlorophyll and carotenoid excitonic couplings in the LH2 system of purple bacteria. *Journal of Physical Chemistry B* **104**, 9540–9553 (2000).

53. T. Mirkovic, A. B. Doust, J. Kim, K. E. Wilk, C. Curutchet, B. Mennucci, R. Cammi, P. M. G. Curmi, G. D. Scholes, Ultrafast light harvesting dynamics in the cryptophyte phycocyanin 645. *Photochemical and Photobiological Sciences* **6**, 964 (2007).

54. A. Ben-Shem, F. Frolow, N. Nelson, Evolution of photosystem i – from symmetry through pseudosymmetry to asymmetry. *FEBS Letters* **564**, 274–280 (2004).

55. D. E. Tronrud, J. Wen, L. Gay, R. E. Blankenship, The structural basis for the difference in absorbance spectra for the FMO antenna protein from various green sulfur bacteria. *Photosynthesis Research* **100**, 79–87 (2009).

56. G. Ritschel, J. Roden, W. T. Strunz, A. Aspuru-Guzik, A. Eisfeld, Absence of quantum oscillations and dependence on site energies in electronic excitation transfer in the fenna–matthews–olson trimer. *The Journal of Physical Chemistry Letters* **2**, 2912–2917 (2011).

57. J. Moix, J. Wu, P. Huo, D. Coker, J. Cao, Efficient energy transfer in light-harvesting systems, III: The influence of the eighth bacteriochlorophyll on the dynamics and efficiency in FMO. *Journal of physical chemistry letters* **2**, 3045–3052 (2011). Publisher: American Chemical Society.

58. Y. Dubi, Interplay between dephasing and geometry and directed heat flow in exciton transfer complexes. *Journal of Physical Chemistry C* **119**, 25252–25259 (2015).

59. S. Hess, M. Chachisvilis, K. Timpmann, M. Jones, G. Fowler, C. Hunter, V. Sundström, Temporally and spectrally resolved subpicosecond energy transfer within the peripheral antenna complex (lh2) and from lh2 to the core antenna complex in photosynthetic purple bacteria. *Proceedings of the National Academy of Sciences* **92**, 12333–12337 (1995).

60. C. D. Van der Weij-De Wit, A. B. Doust, I. H. M. van Stokkum, J. P. Dekker, K. E. Wilk, P. M. G. Curmi, R. van Grondelle, Phycocyanin sensitizes both photosystem i and photosystem II in cryptophyte chroomonas CCMP270 cells. *Biophysical Journal* **94**, 2423–2433 (2008).

61. T. Geyer, V. Helms, Reconstruction of a kinetic model of the chromatophore vesicles from rhodobacter sphaeroides. *Biophysical journal* **91**, 927–937 (2006).

62. S. Scheuring, J. N. Sturgis, V. Prima, A. Bernadac, D. Lévy, J.-L. Rigaud, Watching the photosynthetic apparatus in native membranes. *Proceedings of the National Academy of Sciences* **101**, 11293–11297 (2004).

63. S. Scheuring, J.-L. Rigaud, J. N. Sturgis, Variable lh2 stoichiometry and core clustering in native membranes of rhodospirillum photometricum. *The EMBO journal* **23**, 4127–4133 (2004).

64. M. K. Sener, D. Lu, T. Ritz, S. Park, P. Fromme, K. Schulten, Robustness and optimality of light harvesting in cyanobacterial photosystem i. *The Journal of Physical Chemistry B* **106**, 7948–7960 (2002).

65. G. McDermott, S. Prince, A. Freer, A. Hawthornthwaite-Lawless, M. Papiz, R. Cogdell, N. Isaacs, Crystal structure of an integral membrane light-harvesting complex from photosynthetic bacteria. *Nature* **374**, 517–521 (1995).

66. N. W. Isaacs, R. J. Cogdell, A. A. Freer, S. M. Prince, Light-harvesting mechanisms in purple photosynthetic bacteria. *Current Opinion in Structural Biology* **5**, 794–797 (1995).

67. J. Koepke, X. Hu, C. Muenke, K. Schulten, H. Michel, The crystal structure of the light-harvesting complex ii (b800–850) from rhodospirillum molischianum. *Structure* **4**, 581–597 (1996).

68. J. Dziarmaga, W. H. Zurek, M. Zwolak, Non-local quantum superpositions of topological defects. *Nature Physics* **8**, 49–53 (2012).

69. A. Shabani, M. Mohseni, H. Rabitz, S. Lloyd, Numerical evidence for robustness of environment-assisted quantum transport. *Phys. Rev. E* **89**, 042706 (2014).

70. D. Hayes, J. Wen, G. Panitchayangkoon, R. E. Blankenship, G. S. Engel, Robustness of electronic coherence in the fenna–matthews–olson complex to vibronic and structural modifications. *Faraday discussions* **150**, 459–469 (2011).

71. L. A. Baker, S. Habershon, Robustness, efficiency, and optimality in the fenna-matthews-olson photosynthetic pigment-protein complex. *The Journal of chemical physics* **143**, 09B604_1 (2015).

72. M. Maiuri, E. E. Ostroumov, R. G. Saer, R. E. Blankenship, G. D. Scholes, Coherent wavepackets in the fenna–matthews–olson complex are robust to excitonic-structure perturbations caused by mutagenesis. *Nature chemistry* **10**, 177 (2018).

73. L. A. Pachón, P. Brumer, Physical basis for long-lived electronic coherence in photosynthetic light-harvesting systems. *The Journal of Physical Chemistry Letters* **2**, 2728–2732 (2011).

74. Z. Zhang, J. Wang, Origin of long-lived quantum coherence and excitation dynamics in pigment-protein complexes. *Scientific reports* **6**, 37629 (2016).

Fig. 1. Mechanisms of efficiency-driven evolution and environment-assisted quantum transport (a) Schematic description of the evolutionary progress of photosynthetic complexes towards their current geometry, with efficiency being the evolutionary driving force. As evolution progresses, the structure of the photosynthetic complex evolves towards its current structure (the FMO complex in this example), while increasing efficiency. Is this indeed the evolutionary pathway of photosynthetic complexes, and if so is quantum coherence part of the efficiency enhancement is a central question in the field of quantum biology. (b) Schematic depiction of the population uniformization mechanism shown for a uniform chain of six sites (Blue lines depict the sites in the chain, Yellow arrows show the excitation of first site and extraction from fifth site). The density of the sites are described by blue bars for the quantum regime, ENAQT regime and classical regime, along with a schematic form for the current vs dephasing curves.

Fig. 2. Calculated exciton current as a function of dephasing for the FMO (a) and pc-645 (b) complexes. The shaded Green area indicates the estimated range of physiological dephasing rates. Insets show a schematic description of the exciton complexes (the full Hamiltonians used are provided in the SM section VI).

Fig. 3. Density configuration (i.e. exciton occupation at different sites) of the FMO complex for three different regimes: quantum limit (blue line, $\gamma_{deph} = 10^{-4} \mu s^{-1}$), biological condition (yellow line, $\gamma_{deph} = 10^{6} \mu s^{-1}$) and quantum limit (green line, $\gamma_{deph} = 10^{12} \mu s^{-1}$). The transition from the quantum regime towards the classical regime is accompanied by a shift in the density configuration, from a wave-function-determined configuration to a uniform gradient between the source and sink, with a uniform configuration in between (*26*). To see this more clearly, figures (b)-(c) present the schematic structure of FMO, where each sphere represents a BChl site, and the color brightness reflects its relative density.

Fig. 4. Average LH2 exciton current as a function of dephasing rate (black line), calculated for ≈ 900 possible paths. Pink curves show the current of arbitrary chosen realizations (i.e entry and exit sites) in LH2. Shaded green area marks the natural dephasing rate. Inset: Schematic description of LH2 transfer network (the full Hamiltonian used is provided in the SM section VI).

fig. 5. Current vs dephasing rate for 5000 realizations of FMO-like networks. Energies were kept fixed while hopping matrix elements were picked from a range of $\pm 200 \mathrm{cm}^{-1}$. ENAQT is obtained for almost the same range for all realisations, indicating the independence of efficiency in the ENAQT regime (and the regime itself) on the structure of the system.